Spin-1 Blume–Capel model with longitudinal random crystal and transverse magnetic fields: A mean-field approach

Erhan Albayrak†

Department of Physics, Erciyes University, Kayseri 38039, *Turkey*

(Received 17 December 2012; revised manuscript received 23 February 2013)

The spin-1 Blume–Capel model with transverse Ω and longitudinal external magnetic fields h, in addition to a longitudinal random crystal field D, is studied in the mean-field approximation. It is assumed that the crystal field is either turned on with probability p or turned off with probability $1-p$ on the sites of a square lattice. Phase diagrams are then calculated on the reduced temperature crystal field planes for given values of $\gamma = \Omega/J$ and p at zero h. Thus, the effect of changing γ and p are illustrated on the phase diagrams in great detail and interesting results are observed.

Keywords: random crystal field, transverse field, spin-1, Blume–Capel model

PACS: 75.10.Hk, 75.30.Kz, 75.50.Gg **DOI:** 10.1088/1674-1056/22/7/077501

1. Introduction

The spin-1 Blume–Capel (BC) model includes both bilinear exchange interaction and crystal field terms. The competition between these quantities leads to both the first-order phase transition and a tricritical point. The model is the most interesting, the lowest spin system exhibiting these properties, and therefore has attracted a great deal of attention over the years. After its discovery, it evolved to study many physical systems with different behaviors. The BC model with random crystal field (RCF) is one such a model, and is used, for example, in studying the critical behavior of He^3–He^4 mixtures in random media.[1] Other models include the transverse external magnetic field, transverse Ising model (TIM), which was originally introduced by de Gennes as a pseudo spin model for hydrogen-bonded ferroelectrics.[2]

Randomness may change the critical behavior of a system considerably, therefore, the RCF effects on the BC model were studied using many approximate techniques. For example, the effects of random bonds and RCF interactions were studied in terms of the effective field theory (EFT) with correlations to obtain the phase diagrams of the model.[3] The three distinct types of phase diagrams were calculated within the mean-field approximation (MFA) with RCF, and then different critical behaviors were obtained[4] and its additional ferromagnetic phases and transition lines were obtained by Carneiro *et al.*[5] The effects of RCF on the tricritical behaviors were investigated by the use of EFT with correlations.[6] The RCF effects were investigated on the phase diagrams within the MFA to calculate the phase diagrams.[7] The phase diagrams of the RCF model were obtained by the use of EFT with correlations and comparisons between the EFT, and the MFT results were given.[8] The correlated effective-field (CEF) treatment of the model was carried out on a square lattice and the probability dependence of the tricritical points was studied.[9] The mean-field (MF) version of the spin-1 Ising model for an RCF with a Gaussian probability distribution was examined.[10] The phase diagrams of the model were studied using cluster expansion theory, and the influence of RCF on the phase diagrams at a given concentration of the crystal field was investigated.[11] The phase diagrams of the model in a uniform magnetic field were investigated in the MFT, and the effect of the randomness on the first-order surfaces of the (Δ, T, H) phase diagram was analyzed.[12] The dependence of the phase diagrams on the RCF was investigated for the spin-1 BC model on the Bethe lattice in terms of the recursion relations for the coordination number $Z = 4$, which corresponds to the square lattice.[13] The different versions of the spin-1 RCF model were also studied. The phase diagrams of the two-dimensional BC model with RCF was studied within the framework of a real-space renormalization-group approximation.[14] The Blume–Emery–Griffiths (BEG) model in an RCF in two and three dimensions was studied through a real-space renormalization-group approach and MF approximation, respectively.[15] The random anisotropy BEG model was studied in the pair approximation of the cluster variation method extended to disordered systems.[16]

The transverse field Ising model (TIM) has been used to describe a variety of physical systems. As mentioned above, it was introduced as a pseudo spin model for hydrogen-bonded ferroelectrics, which provides a good description of some of the real anisotropic magnetic materials in a transverse field. An EFT was proposed and used for deriving the phase diagrams of the spin-1 Ising model in the presence of an applied transverse field.[18] The TIM with spin-1 and mixed spins was studied using the discretized path integral representation and the two-spin cluster approximation to obtain the free energy

†Corresponding author. E-mail: albayrak@erciyes.edu.tr

© 2013 Chinese Physical Society and IOP Publishing Ltd

and the critical transverse field of these approximations.[19] The phase diagrams and the tricritical behavior of the TIM with spin-1 were studied using the EFT and the differential-operator technique on the honeycomb lattice, where general expressions for evaluating the second-order phase-transitions and tricritical points in the presence of a crystal field were obtained.[20] The same model was also considered with the dilution of the nearest-neighbor interaction to study the phase diagrams within the framework of the EFT with correlation on a honeycomb lattice.[21] Using the EFT with a probability distribution technique that accounts for the self-spin correlation functions, the phase diagrams and the tricritical points of the transverse spin-1 Ising model with a longitudinal crystal field were investigated on the square lattice,[22] and the influence of site dilution on the tricritical behavior was also studied.[23] The phase diagrams of the spin-1 TIM with the presence of a crystal field were investigated using the EFT, and a method calculating the Gibbs free energy numerically at finite temperature was given.[24] The effect of random bond (site) dilution on the phase transition of a three-dimensional TIM was studied by cluster variation, along with the perturbation expansion method.[25] The critical behavior of a TIM thin film with spin-1 was studied with a correlated EFT treatment.[26] The EFT was used for studying the spin-1 TIM where the lines of critical points in the T–Ω plane, as well as the thermal behavior of all relevant statistical–mechanical quantities, were analyzed for several lattice structures and compared with the standard mean-field predictions.[27] A quantum Ising-like spin-1 model characterized by quadrupolar interaction, coupled to an external anisotropic field with both dipole and quadrupole momenta was analyzed.[28] A spin-1 TIM with longitudinal crystal field in a longitudinal magnetic field was examined by the EFT, including the correlations between different spins that emerge when expanding the identities.[29]

There are also a few studies that combine the TIM with the RCF effects. The phase diagram and magnetic properties of the model are studied using an expansion technique for cluster identities of spin-1 localized spin systems,[30] and the effect of a longitudinal random crystal field interaction on the phase diagrams of the mixed-spin TIM consisting of spin-1/2 and spin-1 is investigated within the finite cluster approximation based on a single-site cluster theory.[31] Thus, in this work, we have also combined the spin-1 TIM with the RCF effects to study the model in terms of a mean-field approximation.[32] To do this, we obtained the necessary equations in the MFA first, and then the form of the random distribution of RCF is applied to these equations to include the RCF for a given transverse magnetic field. The latter is also turned off to study only the RCF effects. As a result, the phase diagrams of the model are obtained in the $(D/J, kT/J)$ plane for a given probability distribution of the crystal field in the range between 0.0 and 1.0 with an increment of $\Delta p = 0.1$ under the effect of an applied transverse magnetic field.

The rest of this work is organized as follows. The next section is devoted to the formulation of the model in terms of the MFA. The last section includes our illustrations and findings in addition to a brief summary and conclusions.

2. Formulation

We consider the spin-1 BC model Hamiltonian given as

$$\mathscr{H} = -J\sum_{\langle i,j\rangle} S_i^z S_j^z - \sum_i D_i (S_i^z)^2 - h\sum_i S_i^z - \Omega\sum_i S_i^x, \qquad (1)$$

where J is the bilinear exchange interaction between the nearest-neighbor (NN) spins, h and Ω are the longitudinal and transverse magnetic fields, respectively, and D_i is the site-dependent crystal field which is distributed according to

$$P(\Delta_i) = p\ \delta(\Delta_i - \Delta) + (1-p)\ \delta(\Delta_i), \qquad (2)$$

with $\Delta_i = D_i/J$. This random distribution of the crystal field, i.e., equation (2), turns the crystal field either on or off randomly for a given probability p on the sites of the lattice. In addition, $\langle i,j\rangle$ indicates the summation over the NN spins. On the other hand, S_i^x and S_i^z are the components of the spin-1 operators at site i, which are given in the matrix form as

$$S_i^x = \frac{1}{\sqrt{2}}\begin{pmatrix} 0 & 1 & 0 \\ 1 & 0 & 1 \\ 0 & 1 & 0 \end{pmatrix} \quad \text{and} \quad S_i^z = \begin{pmatrix} 1 & 0 & 0 \\ 0 & 0 & 0 \\ 0 & 0 & -1 \end{pmatrix}. \qquad (3)$$

Using the mean-field approximation, the $\mathscr{H}$ in Hamiltonian (1) may be expressed in the form

$$-\beta\mathscr{H}_{\rm MFA} = -\beta\sum_i \mathscr{H}_{\rm MFA}^{(i)}, \qquad (4)$$

where

$$-\beta\mathscr{H}_{\rm MFA}^{(i)} = \beta q J S_z S_i^z + \beta D_i (S_i^z)^2 + \beta h S_i^z + \beta\Omega S_i^x, \qquad (5)$$

with $S_z = \langle S_i^z\rangle$, $\beta = 1/(kT)$, k the Boltzmann constant, and q the number of NN spins.

In order to calculate the components of the order parameters, i.e., the dipolar and quadrupolar moments, the partition function is needed, which is given by the definition as

$$\begin{aligned} Z_i &= \mathrm{Tr}_{(i)} \exp(-\beta\mathscr{H}_{\rm MFA}^{(i)}) \\ &= \mathrm{e}^{\lambda_1} + \mathrm{e}^{\lambda_2} + \mathrm{e}^{\lambda_3}, \end{aligned} \qquad (6)$$

where $-\beta\mathscr{H}_{\rm MFA}^{(i)}$ can be represented with the matrix below

$$-\beta\mathscr{H}^{(i)}_{\rm MFA}=\begin{pmatrix}\beta(qJS_z+D_i+h) & \beta\Omega/\sqrt{2} & 0\\ \beta\Omega/\sqrt{2} & 0 & \beta\Omega/\sqrt{2}\\ 0 & \beta\Omega/\sqrt{2} & \beta(-qJS_z+D_i-h)\end{pmatrix}, \tag{7}$$

the eigenvalues of which are the desired λ's in Eq. (6). Thus, the determinant of Eq. (7) yields the eigenvalue equation as

$$\lambda^3+a_2\lambda^2+a_1\lambda+a_0=0, \tag{8}$$

with $a_0=\beta^3\Omega^2D_i$, $a_1=\beta^2(-q^2J^2S_z^2-2qJhS_z+D_i^2-h^2-\Omega^2)$, and $a_2=-2\beta D_i$. The roots of this equation are found from the mathematical identity

$$\lambda_n=2y\cos\left\{\frac{1}{3}\left[\arccos\left(-\frac{G}{2y^3}\right)+2n\pi\right]\right\}-\frac{a_2}{3},\quad n=0,1,2, \tag{9}$$

where $y=(-W)^{1/2}$, $W=(3a_1-a_2^2)/9$, and $G=(27a_0-9a_1a_2+2a_2^3)/27$. After having found the eigenvalues from Eq. (9), one can insert them into Eq. (6) to obtain the explicit form of the partition function. One can now calculate the free energy from

$$f=-\frac{1}{\beta}\ln Z_i, \tag{10}$$

which will be used to obtain the order parameters of the model. Thus, the dipolar moment, or magnetization, along the z axis is given as

$$\begin{aligned}S_z&=\langle S_i^z\rangle=-\frac{\partial f}{\partial h}=\frac{1}{\beta}\frac{\partial\ln Z_i}{\partial h}\\&=\frac{{\rm Tr}_{(i)}[S_i^z\exp(-\beta\mathscr{H}^{(i)}_{\rm MFA})]}{Z_i}\\&=\frac{1}{\beta}\left(\frac{\frac{\partial\lambda_1}{\partial h}e^{\lambda_1}+\frac{\partial\lambda_2}{\partial h}e^{\lambda_2}+\frac{\partial\lambda_3}{\partial h}e^{\lambda_3}}{e^{\lambda_1}+e^{\lambda_2}+e^{\lambda_3}}\right)\\&=\frac{1}{\beta'}\left(\frac{\frac{\partial\lambda_1}{\partial H}e^{\lambda_1}+\frac{\partial\lambda_2}{\partial H}e^{\lambda_2}+\frac{\partial\lambda_3}{\partial H}e^{\lambda_3}}{e^{\lambda_1}+e^{\lambda_2}+e^{\lambda_3}}\right),\end{aligned} \tag{11}$$

where the last term includes $\beta'=\beta J$ and $H=h/J$, which are the reduced temperature and longitudinal external magnetic fields. Similarly, the magnetization along the x axis may be calculated from

$$\begin{aligned}S_x&=\langle S_i^x\rangle=-\frac{\partial f}{\partial\Omega}=\frac{1}{\beta}\frac{\partial\ln Z_i}{\partial\Omega}\\&=\frac{{\rm Tr}_{(i)}[S_i^x\exp(-\beta\mathscr{H}^{(i)}_{\rm MFA})]}{Z_i}\\&=\frac{1}{\beta}\left(\frac{\frac{\partial\lambda_1}{\partial\Omega}e^{\lambda_1}+\frac{\partial\lambda_2}{\partial\Omega}e^{\lambda_2}+\frac{\partial\lambda_3}{\partial\Omega}e^{\lambda_3}}{e^{\lambda_1}+e^{\lambda_2}+e^{\lambda_3}}\right)\\&=\frac{1}{\beta'}\left(\frac{\frac{\partial\lambda_1}{\partial\gamma}e^{\lambda_1}+\frac{\partial\lambda_2}{\partial\gamma}e^{\lambda_2}+\frac{\partial\lambda_3}{\partial\gamma}e^{\lambda_3}}{e^{\lambda_1}+e^{\lambda_2}+e^{\lambda_3}}\right),\end{aligned} \tag{12}$$

with $\gamma=\Omega/J$ the reduced transverse field. Finally, the quadrupolar order-parameter Q_z is obtained from

$$\begin{aligned}Q_z&=\langle(S_i^z)^2\rangle=-\frac{\partial f}{\partial D_i}=\frac{1}{\beta}\frac{\partial\ln Z_i}{\partial D_i}\\&=\frac{{\rm Tr}_{(i)}[(S_i^z)^2\exp(-\beta\mathscr{H}^{(i)}_{\rm MFA})]}{Z_i}\\&=\frac{1}{\beta}\left(\frac{\frac{\partial\lambda_1}{\partial D_i}e^{\lambda_1}+\frac{\partial\lambda_2}{\partial D_i}e^{\lambda_2}+\frac{\partial\lambda_3}{\partial D_i}e^{\lambda_3}}{e^{\lambda_1}+e^{\lambda_2}+e^{\lambda_3}}\right)\\&=\frac{1}{\beta'}\left(\frac{\frac{\partial\lambda_1}{\partial\Delta_i}e^{\lambda_1}+\frac{\partial\lambda_2}{\partial\Delta_i}e^{\lambda_2}+\frac{\partial\lambda_3}{\partial\Delta_i}e^{\lambda_3}}{e^{\lambda_1}+e^{\lambda_2}+e^{\lambda_3}}\right).\end{aligned} \tag{13}$$

We should also note that these equations reduce to the well-known mean field equations for the order parameters along the z axis when the transverse field is turned off, i.e., $\Omega=0$ so $S_x=0$. They are given in terms of the reduced quantities as follows:

$$\begin{aligned}S_z&=\frac{2e^{\beta'\Delta_i}\sinh[\beta'(qS_z+H)]}{1+2e^{\beta'\Delta_i}\cosh[\beta'(qS_z+H)]},\\Q_z&=\frac{2e^{\beta'\Delta_i}\cosh[\beta'(qS_z+H)]}{1+2e^{\beta'\Delta_i}\cosh[\beta'(qS_z+H)]}.\end{aligned} \tag{14}$$

It should be mentioned that in order to include the effects of the RCF, one has to take the average of the above order parameters over the random crystal field distribution, i.e., Eq. (2).

3. Results and discussion

In this section, we illustrate the phase diagrams in the $(\Delta,kT/J)$ plane for given values of γ when p is varied from 0.0 to 1.0 with the increment of 0.1. In the figures, the second-order ($T_{\rm c}$) and first-order ($T_{\rm t}$) phase transition lines are indicated with solid and dashed lines, respectively, and are obtained from the thermal behaviors of magnetization. The tricritical point at which the $T_{\rm c}$ and $T_{\rm t}$ lines combine are indicated with solid triangles. It should be noted that the model reduces to the spin-1 BC model when $\gamma=0.0$ and $p=1.0$, the RCF spin-1 BC model for $\gamma=0.0$ when $0.0<p<1.0$, and the spin-1 Ising model with only J when p or Δ is equal to zero and $\gamma=0.0$.

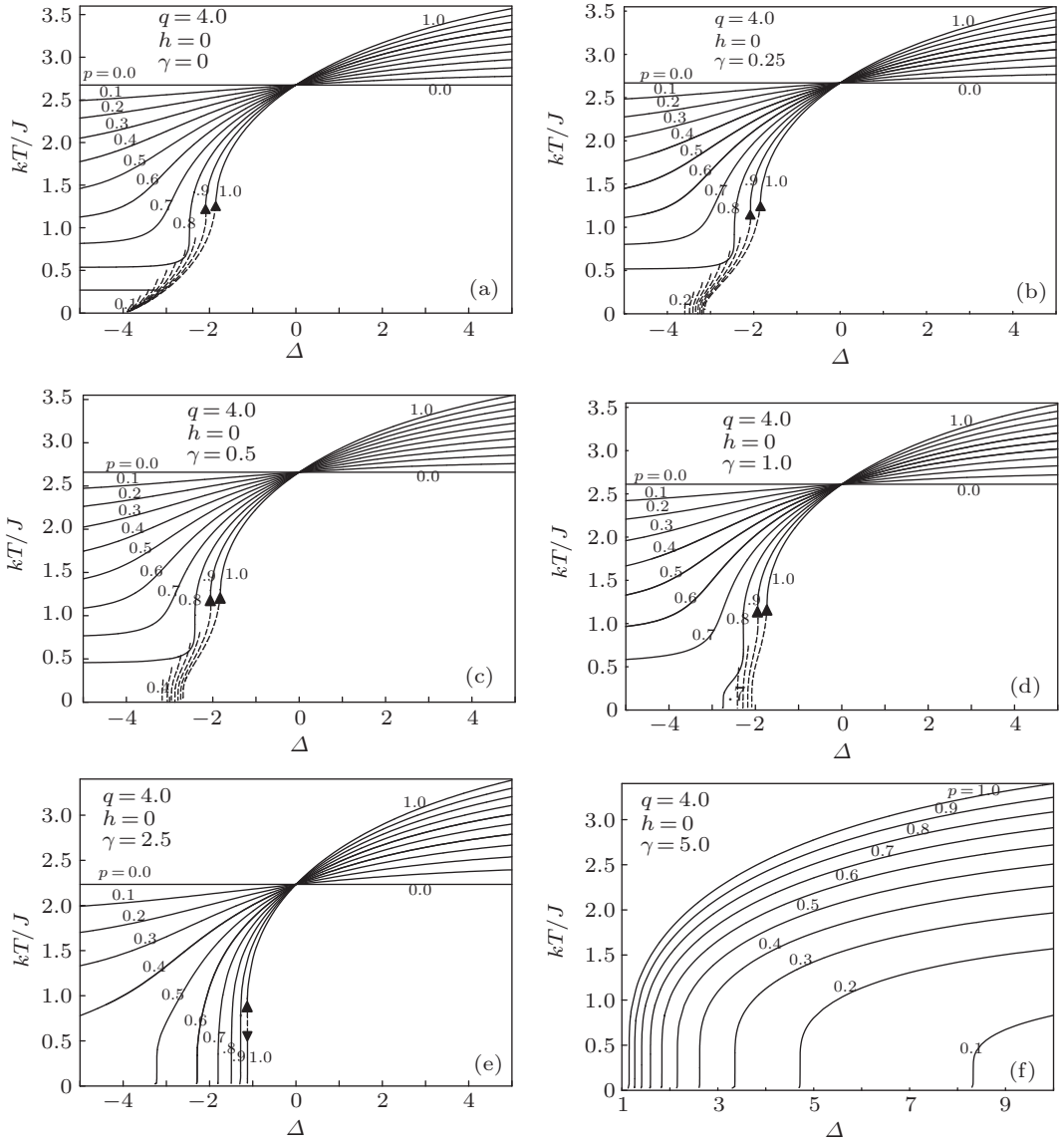


Fig. 1. The phase diagrams on the $(\Delta, kT/J)$ planes for $p = 0.0$ to 1.0 with the increment of 0.1 when (a) $\gamma = 0.0$, (b) $\gamma = 0.25$, (c) $\gamma = 0.5$, (d) $\gamma = 1.0$, (e) $\gamma = 2.5$, and (f) $\gamma = 5.0$.

Figure 1(a) is obtained for $\gamma = 0.0$, i.e., the RCF spin-1 BC model. When $p = 0.0$, which also means that the crystal field is turned off for all sites, the T_c line is just a straight line. When $p = 1.0$, the model is only a spin-1 BC model with all sites under the effect of a constant crystal field. The phase line is the one with the T_c- and T_t-lines combined at the tricritical point, which is a very well-known behavior. The higher p is, the higher the temperatures of the T_c-lines are when $\Delta > 0.0$. It is exactly the opposite for $\Delta < 0.0$, and all of the T_c-lines combine at $\Delta = 0.0$ as expected. They become constant in temperature for higher $|\Delta|$ values. The T_t-lines are shorter and are seen at lower negative Δ for lower p, which terminates at the isolated points. The temperatures of the isolated points are higher for higher p's. When p =0.9 and 1.0, they terminate at the tricritical points. The temperature of the latter is higher, as seen from the figure. In the $\Delta < 0.0$ region, no T_c-line exists for $p = 1.0$ and a straight T_c-line at low temperature combined with the T_t-line at the critical end point is found for $p = 0.9$, which is similar to Fig. 2 of Ref. [5]. It is also clear that all the T_t-lines emerge from the same Δ at zero temperature. Note also that our Fig. 1(a) is quite different from the Fig. 2 of the Bethe lattice treatment of the same model in Ref. [32]. This may be caused by the application procedure of the RCF on a given lattice. In this paper, we take an average over the probability distribution for the calculation of the order parameters. However, in the Bethe lattice case, one starts from the central spin, where the CF is either turned on with p or off with $1 - p$, and then goes to the second-spin, i.e., the nearest-neighbor of the central one, and again turns on or off the crystal field with same p and $1 - p$, respectively, and so on. The latter includes randomness in a more realistic way than the previous one. Thus the obvious difference in the phase diagrams appears.

Figure 1(b) is obtained for $\gamma = 0.25$, which presents similar behaviors as the previous figure. But now, the temperatures of the critical lines are lower in comparison, which is more obvious for higher p's at lower negative Δ's. The T_c-line for $p = 0.9$ when $\Delta < 0.0$ vanishes, and therefore the critical end point disappears. The T_t-lines do not emerge from the same Δ at zero temperature for each p. Instead, they emerge from lower negative Δ values for lower p's. They are also shortened and the T_t-line for $p = 0.1$ even vanishes. Figures 1(c) and (d) are obtained for $\gamma = 0.5$ and $\gamma = 1.0$, respectively. Upon increasing the values of γ, the temperatures of the critical lines further decrease. The T_t-lines for $p = 0.2$ to 0.3 when $\gamma = 0.5$ and the T_t-lines for $p = 0.2$ to 0.6 when $\gamma = 1.0$ vanish. Figure 1(e), obtained for $\gamma = 2.5$, shows that the T_c-lines from 0.5 to 1.0 terminate at zero temperature at finite negative Δ. The tricritical point for $p = 0.9$ vanishes. However, we see two tricritical points for $p = 1.0$. The stable and unstable ones are indicated with upward and downward triangles, respectively. Figure 1(f), obtained for $\gamma = 5.0$, shows that all the T_t-lines disappear and only the T_c-lines are left in the phase diagram, which is similar to Fig. 1 of Ref. [23]. No more critical lines are seen in the negative Δ values and all the T_c-lines terminate at zero temperature at lower finite positive Δ values for higher p's. Thus, as γ increases, all the lines shift to the positive Δ values, as seen from all the phase diagrams. The lower the p is, the more a shift to the right is illustrated. All these figures show that there is a strong competition between γ and negative Δ. The lower p means that a lower number of sites are under the influence of Δ. Therefore, the critical lines are at higher temperatures for lower p, since the competition is weak between γ and negative Δ. For higher p, the competition is strong, thus the T_c-lines bend towards the right and terminate at zero temperature at some finite values of Δ for higher γ.

4. Conclusion

In summary, we have examined the spin-1 Blume–Capel model with transverse and longitudinal external magnetic fields, in addition to a longitudinal random crystal field, in the mean-field approximation. We also assumed that the crystal field was either turned on with a probability p or turned off with a probability $1 - p$ on the sites of a square lattice. The calculated phase diagrams revealed that there is strong competition between γ and negative Δ values, which leads to the disappearance of the critical lines for $\Delta < 0$. The competition still exists for positive Δ, but now the T_c-lines are shifted to higher Δ values. It is found that the model exhibits tricritical points, stable and unstable ones, critical end points and isolated points. Finally, we should note that there is no work in the literature with which we can directly compare our results for the RCF spin-1 TIM.

References

[1] Maritan A, Cieplak M, Swift M R, Toigo F and Banavar J R 1992 *Phys. Rev. Lett.* **69** 221
[2] de Gennes P G 1963 *Solid State Commun.* **1** 132
[3] Kaneyoshi T 1986 *J. Phys. C: Solid State Phys.* **19** L557
[4] Benyoussef A, Biaz T, Saber M and Touzani M 1987 *J. Phys. C: Solid State Phys.* **20** 5349
[5] Carneiro C E I, Henriques V B and Salinas S R 1989 *J. Phys.: Condens. Matter* **1** 3687
[6] Kaneyoshi T 1988 *J. Phys. C: Solid State Phys.* **21** L679
[7] Boccara N, Elkenz A and Saber M 1989 *J. Phys.: Condens. Matter* **1** 5721
[8] Kaneyoshi T and Mielnicki J 1990 *J. Phys.: Condens. Matter* **2** 8773
[9] Kaneyoshi T 1992 *Phys. Status Solidi (b)* **170** 313
[10] Carneiro C E I, Henriques V B and Salinas S R 1990 *J. Phys. A: Math. Gen.* **23** 3383
[11] Ilkovič V 1995 *Phys. Status Solidi (b)* **192** K7
[12] Borelli M E S and Carneiro C E I 1996 *Physica A* **230** 249
[13] Albayrak E 2011 *Physica A* **390** 1529
[14] Branco N S and Boechat B M 1997 *Phys. Rev. B* **56** 11673
[15] Branco N S 1999 *Phys. Rev. B* **60** 1033
[16] Buzano C, Maritan A and Pelizzola A 1994 *J. Phys.: Condens. Matter* **6** 327
[17] Ananikian N S, Avakian A R and Izmailian N S 1991 *Physica A* **172** 391
[18] Sarmento E F, Fittipaldi I P and Kaneyoshi T 1992 *J. Magn. Magn. Mater.* **104** 233
[19] Dai S T, Jiang Q and Li Z Y 1990 *Phys. Rev. B* **42** 2597
[20] Jiang X F, Li J L, Zhong J L and Yang C Z 1993 *Phys. Rev. B* **47** 827
[21] Jiang X F 1994 *J. Magn. Magn. Mater.* **134** 167
[22] Htoutou K, Benaboud A, Ainane A and Saber M 2004 *Physica A* **338** 479
[23] Htoutou K, Oubelkacem A, Ainane A and Saber M 2005 *J. Magn. Magn. Mater.* **288** 259
[24] Miao H, Wei G, Liu J and Geng J 2009 *J. Magn. Magn. Mater.* **321** 102
[25] Saxena V K 1983 *Phys. Rev. B* **27** 6884
[26] Zhong J L, Yang C Z and Li J L 1991 *J. Phys: Condens. Matter* **3** 1301
[27] Fittipaldi I P, Sarmento E F and Kaneyoshi T 1992 *Physica A* **186** 591
[28] Buzano C and Vadacchino M 1983 *Z. Phys. B: Condens. Matter* **53** 63
[29] Yuksel Y and Polat H 2010 *J. Magn. Magn. Mater.* **322** 3907
[30] Benyoussef A and Ez-Zahraouy H 1994 *J. Phys.: Condens. Matter* **6** 3411
[31] Benayad N, Zerhouni R and Klümper A 1998 *Eur. Phys. J. B* **5** 687
[32] Albayrak E and Keskin M 1999 *J. Magn. Magn. Mater.* **206** 83